ARTICLE NO. 78-141

Inlet and Duct for the QSRA Boundary-Layer Control System

Daniel W. Gunnarson*
Boeing Commercial Airplane Company, Seattle, Wash.
and
Jack C. McArdle†
NASA Lewis Research Center, Cleveland, Ohio

An important requirement for the successful operation of the boundary-layer control (BLC) system for the quiet short-haul research airplane (QSRA) was to provide a source of pressurized airflow for BLC use. This was successfully achieved by 1) positioning a BLC inlet in the engine fan duct in a region of high local total pressure, and 2) carefully contouring the BLC inlet and duct. Potential flow with boundary layer analysis techniques was used as an aid to select the inlet and duct geometries. Airflow and total pressure profile test data were obtained. These data showed that the required total pressure of more than 99% of the average fan duct total presure was achieved.

Nomenclature

Bm	= momentum thickness of boundary layer
C_f	= skin friction coefficient
D	= distance across BLC duct from top wall to bottom wall in bending plane
$L.E.$	= leading edge of inlet lip
M	= Mach number
N_F	= fan speed in revolutions per minute
R	= radius of curvature in bending plane
W	= weight flow rate
X	= horizontal coordinate of BLC duct
Y	= vertical coordinate of BLC duct
θ	= ratio of temperature to standard temperature (518.7°R)
δ	= ratio of pressure to standard pressure (2116 psf)

Subscripts

avg	= average
BLC	= pertaining to flow in duct supplying air to the boundary layer control (BLC) system
F	= engine fan
$f.d.$	= fan duct
ej	= at entrance to ejector which is the downstream end of BLC duct
ent	= at entrance to BLC inlet
L	= local
t	= total
thr	= at throat of BLC inlet
0	= at station ahead of engine inlet
2	= station at entrance to engine fan

Introduction

THE QSRA (Quiet Short Haul Research Airplane) is an experimental airplane which The Boeing Company is modifying for the NASA Ames Research Center.[1] As shown in Fig. 1, four AVCO Lycoming YF 102 turbofan engines exhaust over the wing. With flaps deflected this provides lift augmentation by turning the engine exhaust downward and inducing airflow over the wing.

Additional lift and control are provided by blown leading edges and ailerons. The associated BLC (Boundary Layer Control) system used approximately 3% of the engine fan flow. At approach engine thrust, the fan duct bleed is supplemented with engine compressor bleed. The two streams are mixed in an ejector which feeds the aircraft BLC system as shown in Fig. 2.

To operate properly, the BLC system required reasonably high total pressure at the discharge locations. The BLC ducting system between the ejector (see Fig. 2) and the discharge nozzles had duct diameters and bend radii consistent with the available space. The result was that almost all of the permissible BLC system pressure loss occurred downstream of the ejector. Therefore, the BLC inlet and duct ahead of the ejector had to provide airflow with more than 99% of the average fan duct total pressure.

The BLC inlet and duct must diffuse the airflow from high engine fan duct velocities to much lower velocities at the ejector entrance. When combined with space limitations which necessitated an S-shaped flow duct, the BLC requirement for airflow having 99% of fan duct total pressure presented a difficult design task.

Geometric constraints forced the BLC inlet to be downstream of the fan engine exit flange. Also the exit of the BLC inlet duct had to be located far enough forward to provide space for the BLC ejector and its associated ducting. This led to a BLC inlet duct with curves in both the vertical and horizontal planes as illustrated in Fig. 3.

Theoretical Flow Analysis

Flow Analysis Approach

Potential flow and boundary-layer analyses were used to analyze the flow throughout the inlet and upstream of the inlet on the fan duct walls. Although the problem is three-dimensional, a two-dimensional approximation was applied. This approach is less exact but avoids programming the complex three-dimensional geometry and avoids the long and expensive computing times associated with presently available three-dimensional flow analysis programs. The selected computer program combined the potential flow solution[2] with a wall boundary-layer analysis[3] to provide an assessment of boundary-layer characteristics. Previously measured fan duct flow data were used to estimate upstream duct wall

Presented as Paper 78-141 at the AIAA 16th Aerospace Sciences Meeting, Huntsville, Ala., Jan. 16-18, 1978; submitted Feb. 14, 1978; revision received Aug. 18, 1978.

Index categories: Subsonic Flow; Airbreathing Propulsion; Subsystem Design.

*Senior Specialist Engineer, Propulsion Technology Staff.
†Aerospace Engineer.

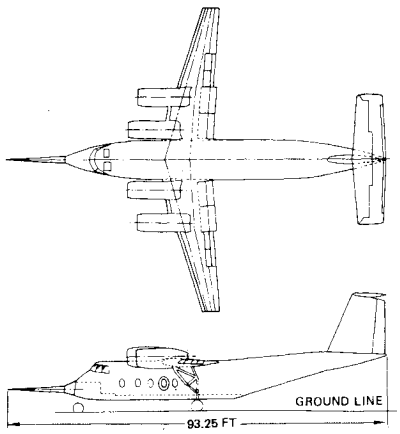

Fig. 1 QSRA airplane configuration.

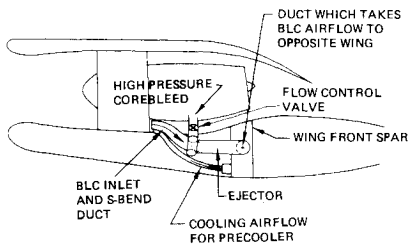

Fig. 2 QSRA nacelle showing BLC airflow supply system.

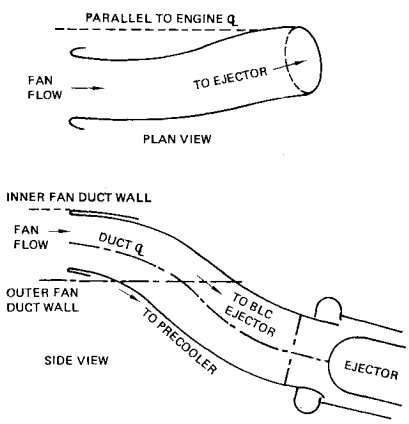

Fig. 3 Two views of BLC inlet and duct.

boundary-layer characteristics, shape factor, and thickness (e.g., see Fig. 17). Avoidance of boundary-layer separation (in the BLC inlet and/or on the fan duct walls) was the acceptance criterion used in the analysis.

BLC Inlet Concepts Analyzed

Three conceptual BLC inlet duct configurations were investigated as shown in Fig. 4. In configuration I shown in Fig. 4a the inlet spans the fan duct from inner to outer wall. It therefore ingests the boundary layer from the fan duct walls. The S-bend duct from inlet to exit is constant area, so there was no diffusing within the duct. Diffusion of the BLC airflow from the fan duct Mach number of 0.54 to the inlet Mach number of 0.3 occurred in the fan duct ahead of the inlet lip.

The inlet of configuration II shown in Fig. 4b also spans the fan duct and ingests fan duct boundary layer. However, the flow area at the inlet station is somewhat smaller than in configuration I. Also, the flow diffuses in the S-bend duct from Mach 0.4 at the inlet to Mach 0.3 at the exit. Diffusion from the fan duct Mach of 0.54 to the inlet Mach of 0.4 occurred ahead of the inlet lip.

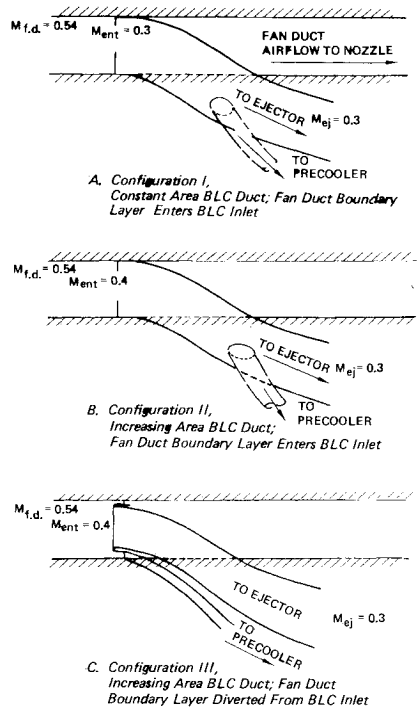

Fig. 4 BLC inlet S-bend configuration concepts.

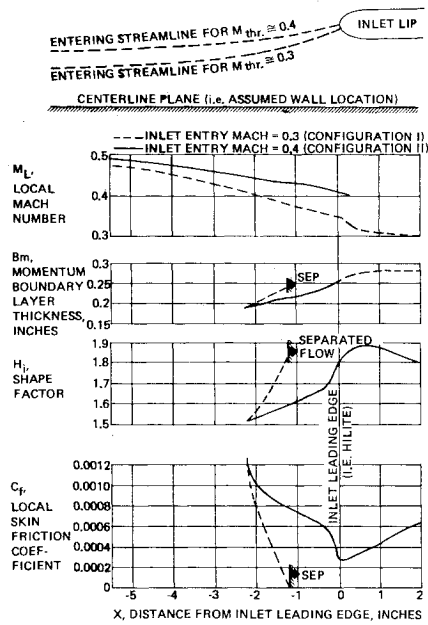

Fig. 5 Boundary-layer parameters on bottom fan duct wall ahead of the BLC inlet.

The inlet of configuration III shown in Fig. 4c is sized and located so that fan duct boundary-layer air does not enter the BLC inlet. Air entering the inlet diffuses in the engine fan duct from Mach 0.54 to about Mach 0.4, and then to Mach 0.3 in the BLC duct. This configuration utilizes the ECS (Environmental Control System) requirement for about 0.4% of the inboard engine airflow for cooling. Airflow near the outer fan duct wall was ducted to the ECS cooler instead of the BLC inlet. Lower-energy airflow is adequate for ECS cooling purposes.

Design and packaging considerations favored configuration I or II because either of these resulted in a simpler installation than configuration III. Therefore, they were analyzed first to determine if their flow characteristics were satisfactory.

Analysis of Fan Duct Boundary Layer Ahead of BLC Inlet

Because considerable diffusion occurred in the fan duct ahead of the inlet, the initial study focused on the fan duct wall boundary layer. The single-stage fan was about 24 in. upstream from the BLC inlet. Transition from laminar to turbulent boundary layer occurred on the fan duct walls 20 in. or more ahead of the BLC inlet.

Calculated boundary-layer shape factor and local skin friction coefficient are shown in the lower two plots of Fig. 5. These parameters indicate boundary-layer attachment or separation potential. When the shape factor increases to approximately 1.8, flow separation is imminent. A negative local skin friction coefficient indicates that the flow velocity near the wall has reversed direction and has separated.

The dashed curves of Fig. 5 show flow and boundary-layer characteristics for BLC inlet duct configuration I, and the solid curves show these for configuration II. Separation of the fan duct boundary layer occurred 1.2 in. ahead of the BLC inlet lip for configuration I. No separation occurred in the fan duct with configuration II. However, shape factors over 1.8 near the inlet lip of configuration II show that near-separation conditions existed there.

Flow Analysis of Configuration II Inside BLC Duct

Although configuration II was unseparated in the fan duct ahead of the BLC inlet, separation was still possible within the BLC duct. Therefore, the flow was analyzed through the BLC duct of configuration II. The results of this analysis showed that separation is predicted to occur on the bottom duct wall about 13 in. from the inlet throat. Also, near-separation conditions exist on the top wall 5 in. from the inlet lip. Configurations I and II were rejected because the flow analysis indicated boundary-layer separation would occur either on the fan duct wall ahead of the inlet or within the S-bend of the duct.

Geometry of Selected BLC Inlet Configuration

Configuration III does not allow fan duct boundary-layer air to enter the inlet. Diffusion occurs both in the fan duct ahead of the inlet and within the duct as shown in Fig. 4c. Inlet lip contours are shown in Fig. 6. These contours were chosen so that separation or shock waves would not form on external or internal inlet surfaces.

The contours in the S-bend portion of the inlet had to be such that separation did not occur in the S-bend shaped diffuser duct. High diffusion rates with separation-free flow are possible if the boundary layer is thin. Therefore, the inlet walls can have high turning rates near the entry where the boundary layer is still thin. This was demonstrated during the development of a similar inlet for the air-launched cruise missile.[4] The contour lines used for the three inlet duct configurations analyzed herein were based on the contours of the inlet in Ref. 4. The lines were modified to fit the geometric constraints of the QSRA installation.

Figure 7 shows the QSRA S-bend duct radius of curvature ratio and the area progression along the duct centerline. Duct design definition was simplified by changing curvature radii in steps as shown in Fig. 7, even though flow theory indicates duct radius of curvature changes should be gradual. Subsequent analysis and test data indicate any adverse effect of stepwise changes in curvature to be very small.

Flow Analysis Results of Selected BLC Inlet Configuration

The two-dimensional geometry used in the analysis and the results of the flow analysis of configuration III are shown in

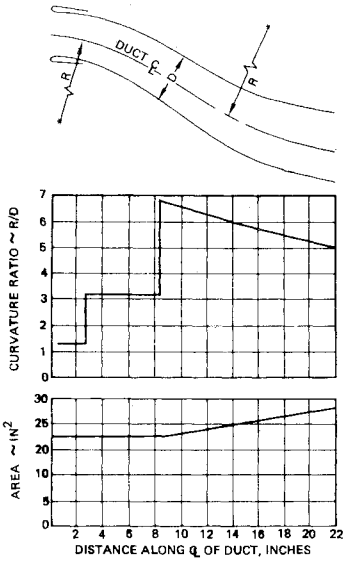

Fig. 7 BLC S-bend duct area and radius of curvature plots.

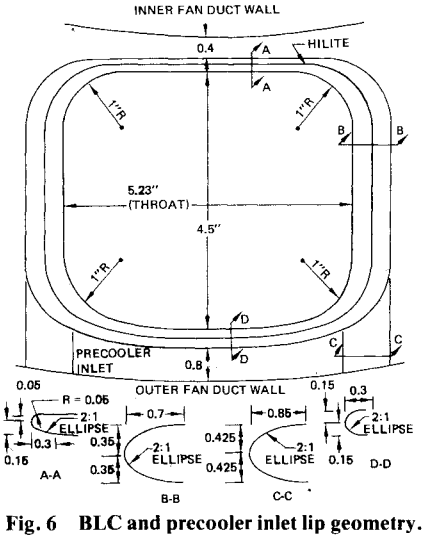

Fig. 6 BLC and precooler inlet lip geometry.

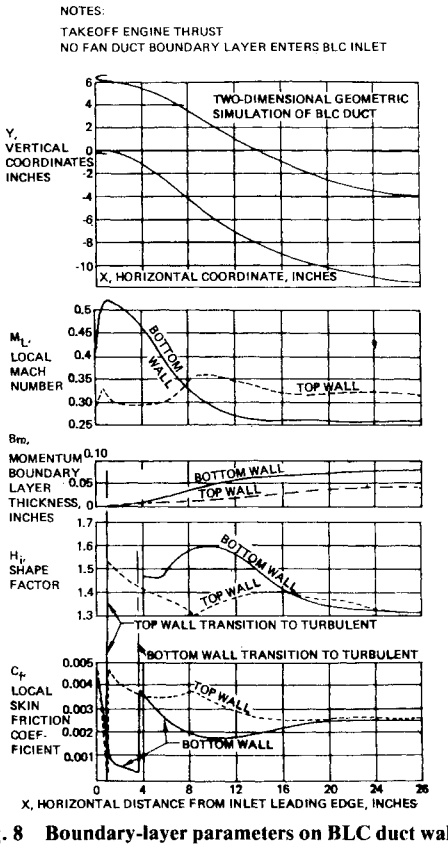

Fig. 8 Boundary-layer parameters on BLC duct walls.

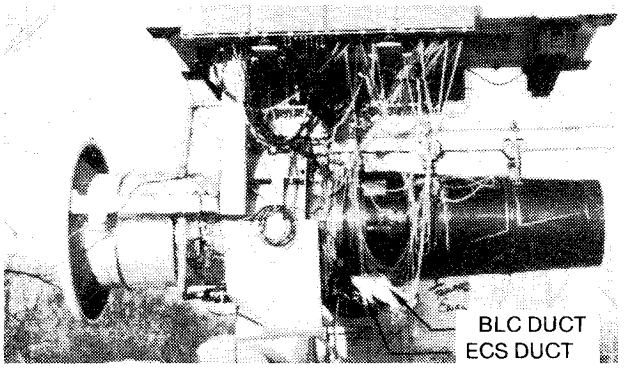

Fig. 9 YF-102 engine mounted on test stand.

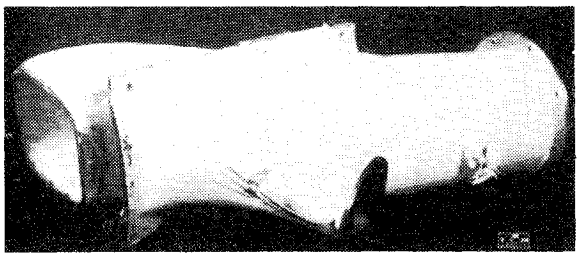

Fig. 10 BLC inlet duct before being installed on engine.

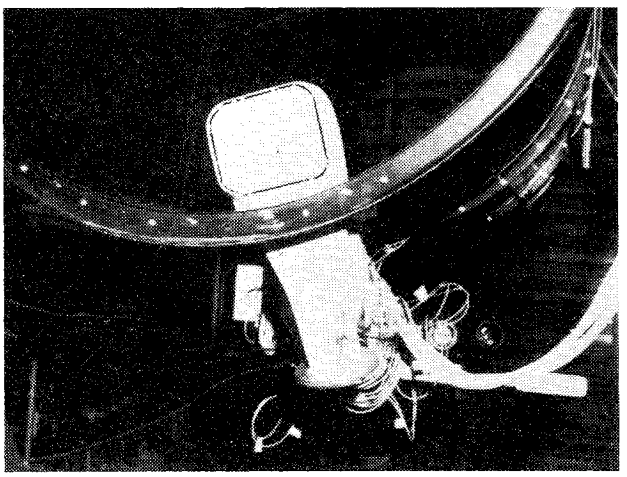

Fig. 11 BLC inlet duct installed in fan duct (fan duct unbolted from engine).

Fig. 8. Flow and boundary-layer parameters for the top and bottom duct surfaces are shown at takeoff engine thrust setting. The shape factor and friction coefficient plots in Fig. 8 show that there is no problem of flow separation. The boundary-layer flow in the BLC duct was also analyzed and found to remain attached at approach engine thrust setting.

The two-dimensional analysis, therefore, shows this to be a satisfactory inlet and duct design. However, two-dimensional analysis does not address secondary airflow behavior near the corners of the duct. Large corner radii in a rectangular duct are known to reduce secondary airflow problems. Therefore, corner radii equal to about 20% of the duct width were used as shown in Fig. 6.

Test

A test of the engine with the BLC inlet duct installed was made at the NASA Lewis Research Center. The test measured the total pressure of the BLC airflow and determined if the BLC inlet duct installation adversely affected engine operation.

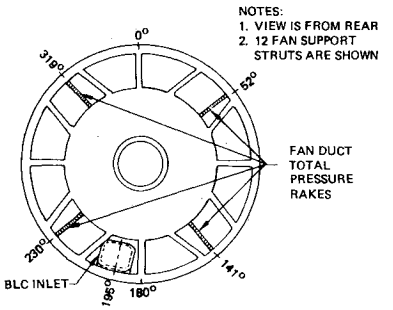

Fig. 12 Location of BLC inlet and total pressure probes in fan duct.

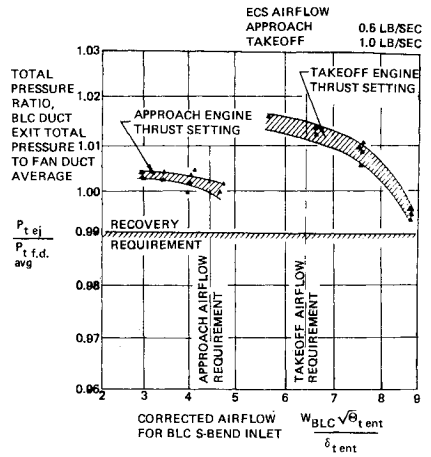

Fig. 13 BLC inlet duct total pressure ratio.

Test Concept and Configuration

The model duct and installation parts built by the NASA Ames Research Center were then fitted by the NASA Lewis Research Center to a YF102 test engine. The YF102 engine mounted on the test stand is shown in Fig. 9, the BLC inlet duct before being installed is shown in Fig. 10, and the BLC inlet in the fan duct wall before the fan duct was bolted onto the engine flange is shown in Fig. 11. The inlet was positioned circumferentially in the fan duct so that its centerline was at 195 deg clockwise when viewed from the rear. In this location the inlet is between two fan support struts as shown in Fig. 12.

A series of nozzle sizes were fitted to the BLC duct exit and the ECS duct exit. The proper range of BLC and ECS airflows were obtained in this way. For each BLC and ECS nozzle combination the engine was run at the full range of fan speeds which provided a complete matrix of engine conditions and BLC airflows.

Instrumentation

Fan duct total pressure distribution was recorded using 40 pressure probes on four rakes installed in the fan duct as shown in Fig. 12. The arithmetic average of these probes provided the average fan duct total pressure for these tests. This was not the average total pressure of the air entering the BLC inlet but gave a useful measurement to relate the BLC duct exit pressure with the corresponding engine condition.

Static pressure pickups were located along the upper and lower surfaces of the BLC inlet duct. At the exit of the BLC inlet duct was an equi-area 17-probe total pressure rake. Two additional boundary-layer probes were located between the outer equi-area probe and the wall. Four wall static pressure pickups were located at 90 deg intervals around the periphery of the BLC duct exit.

Five equi-area total pressure probes were located at the exit of the ECS duct. Flow through the BLC duct and the ECS duct was both controlled and measured by using a series of conical exit nozzles having different throat areas.

Instrumentation and Data Accuracy

Data for each test point were recorded during a 36-s period in which two full scans of data were obtained. Strip charts showed that fan speed could vary as much as 3% during the recording time. Variations were due principally to gusts and crosswinds which occurred at the engine inlet and exit for some tests. To minimize errors from fan speed variations, data points were repeated when large variations were observed on the strip charts. The repeated data points were processed individually and are shown as separate points on the graphs.

As stated previously, fan duct total pressure is the average of 40 individual measurements in the duct, and the BLC duct total pressure is the average of 17 individual measurements. The estimated accuracy for each individual measurement is ± 0.05 psi. Individual total pressure ratios could thus have an inaccuracy of as much as 0.65%, but this is very improbable.

Test Results

Engine Operation

The engine operated satisfactorily at all conditions with the BLC and ECS inlet ducts installed.

Total Pressure Ratio of BLC Inlet Duct

The ratio of BLC duct exit total pressure to average fan duct total pressure is shown as a function of BLC airflow in Fig. 13. These data show the BLC total pressure ratio to be 1.00 when matched at the approach condition and 1.01 when matched at the takeoff condition. The reasons for these high total pressure ratios are discussed later.

Distortion of BLC Inlet Duct

The total pressure distortion at the BLC inlet duct exit is shown in Fig. 14. At the takeoff and approach conditions the total pressure distortion is very low (i.e., less than 5%). Distribution of Mach number at the BLC inlet duct exit at approach and takeoff is shown in Fig. 15. The relatively flat velocity profile at the exit from the BLC inlet duct will allow the ejector to operate efficiently.

BLC Total Pressure Characteristics Discussion

The effect of engine fan speed on total pressure ratio in the BLC duct is shown in Fig. 16. The upper curve of Fig. 16 is the ratio of BLC duct exit total pressure to average fan duct total pressure. The lower curve of Fig. 16 is the ratio of BLC duct exit total pressure to the estimated total pressure at the BLC inlet in the fan duct. The difference between the two curves of Fig. 16 is illustrated by Fig. 17. The fan duct total pressure profiles in Fig. 17 show that the BLC inlet uses only the choice center air. This is the reason the BLC duct total pressure is often higher than the average fan duct total pressure.

The estimated total pressure recovery of the BLC inlet duct as shown in the lower curve of Fig. 16 is also very high. Therefore, the very high BLC duct total pressure is because of two reasons: 1) the pressure loss in the BLC inlet duct is very low, and 2) the BLC inlet is positioned in the engine fan duct outside the fan duct boundary layer and between fan support struts. In this location the BLC inlet receives airflow with higher than average fan duct total pressure.

The ratio of BLC duct total pressure to fan duct average total pressure is higher at high fan rpm's than at low fan rpm's for the following reasons: 1) as shown in Fig. 17 at the high engine fan speed, the total pressure of the center portion of the fan duct air is much higher relative to the entire fan duct airflow than is true at the lower fan speed, and 2) a larger portion of the fan duct airflow enters the BLC inlet at low fan speed than at high fan speed. This means some low-energy

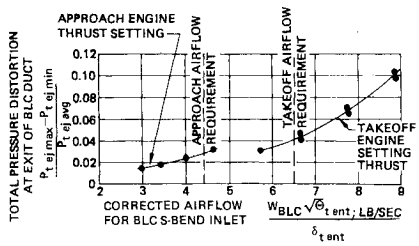

Fig. 14 Total pressure distortion at end of BLC duct.

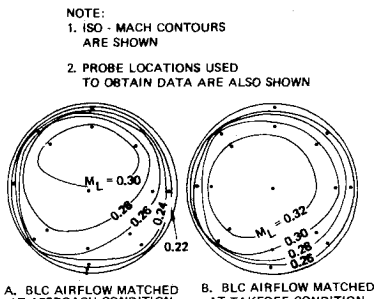

Fig. 15 Distribution of Mach number at exit of BLC duct.

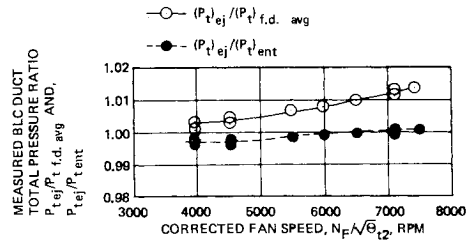

Fig. 16 Effect of fan duct pressure average choice on measured pressure ratio in BLC duct.

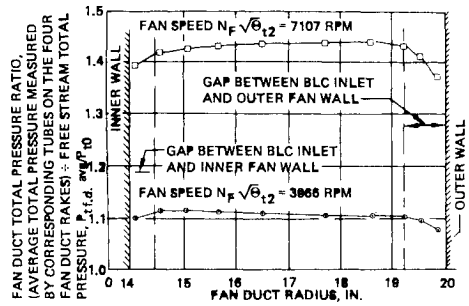

Fig. 17 Total pressure profile in fan duct.

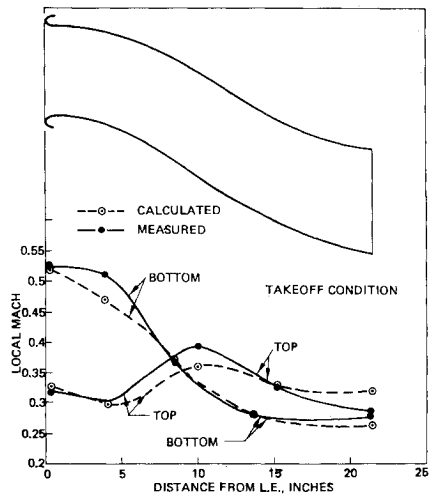

Fig. 18 Comparison of test with theoretically computed local Mach numbers along the duct wall.

bondary layer or strut wake airflow is more likely to enter the BLC inlet at low fan speeds than at high fan speeds.

Comparison of Calculated and Measured Duct Wall Mach Numbers

Measured local Mach numbers on the BLC duct walls were calculated using measured local static pressure and average fan duct total pressure. Measured Mach numbers are compared with previously computed local Mach numbers in Fig. 18. The agreement is quite good. The small differences between the calculated and test data are probably because the two-dimensional geometry used in the analysis was not completely representative. Also the test model probably had surface slope differences near some of the static pressure pickups.

Conclusions

1) The BLC inlet and duct for the QSRA as designed produced airflow with exceptionally high total pressure.

2) Two-dimensional potential flow and boundary layer analysis techniques were used to choose the BLC inlet and duct design. Test results validated that a satisfactory design was chosen.

3) The ratio of total pressure at the BLC inlet duct exit to the average fan duct total pressure was near or above 1.00. The two reasons for this were a) the BLC inlet intake was correctly located in a region of higher than average fan duct total pressure, and b) the pressure loss in the BLC duct is very low.

Acknowledgments

This work was sponsored by the NASA Ames Research Center as part of the quiet shorthaul research airplane (QSRA) development program. Tests with the YF102 engine were conducted by NASA at the Lewis Research Center.

References

[1] "Quiet Propulsive Lift Research Aircraft Design Study," NASA CR-137557, Oct. 1974.

[2] Colehour, J. L., "Transonic Flow Analysis Using a Streamline Coordinate Transformation Procedure," AIAA Paper 73-657, Palm Springs, Calif., July 1973.

[3] Reyhner, T. A., "Finite Difference Solution of the Compressible Turbulent Boundary Layer Equations," *Proceedings; Computation of Turbulent Boundary Layers-1968 AFOSR-IFP-Stanford Conference*, Vol. I; edited by S. J. Kline, et al., Stanford University, 1969, pp. 375-383.

[4] Brunner, D. W., Marshall, F. L., Marrs, K. J., Edwards, R. W., and Pascoe, R. A., "Development of the Integrated Propulsion System for the AGM-86A Air-Launched Cruise Missile," AIAA Paper 76-916, Dallas, Texas, Sept. 1976.